DR ZHAO WANG (Orcid ID : 0000-0001-5431-1785)

DR PENG ZHAN (Orcid ID : 0000-0002-9675-6026)

PROFESSOR XINYONG LIU (Orcid ID : 0000-0002-5833-3807)

Article type : Research Article

Correponding author mail id: xinyongl@sdu.edu.cn

Discovery of potent HIV-1 non-nucleoside reverse transcriptase inhibitors by exploring the structure-activity relationship of solvent-exposed regions I

Dongwei Kang,[†] Zhao Wang,[†] Meng Chen,[|] Da Feng,[†] Gaochan Wu,[†] Zhongxia Zhou,[†] Lanlan Jing,[†] Xiaofang Zuo, [†] Xiangyi Jiang, [†] Dirk Daelemans,[§] Erik De Clercq, [§] Christophe Pannecouque, [§] Peng Zhan,[†,*] and Xinyong Liu[†,*]

[†]*Department of Medicinal Chemistry, Key Laboratory of Chemical Biology (Ministry of Education), School of Pharmaceutical Sciences, Shandong University, 44 West Culture Road, 250012 Jinan, Shandong, PR China*

[|]*Shandong Center for Disease Control and Prevention, 250014 Jinan, Shandong, PR China*

[§]*Rega Institute for Medical Research, K.U.Leuven, Minderbroedersstraat 10, B-3000 Leuven, Belgium*

ABSTRACT:

Two novel series of human immunodeficiency virus-1 (HIV-1) non-nucleoside reverse transcriptase inhibitors (NNRTIs) bearing a thiophene[3,2-*d*]pyrimidine scaffold and sulfonamide linker in the right wing have been identified, which demonstrated with active potency against wild-type (WT) HIV-1 strain in MT-4 cells with inhibitory concentrations ranging from micromolar to submicromolar. Especially, against the mutant strains K103N and E138K, most compounds exhibited more potent activity than against WT HIV-1. Compound **7** (EC_{50} = 0.014, 0.031 μM) achieved the most potent activity against the two mutations, being more effective than that of nevirapine (NVP, EC_{50} = 7.572, 0.190 μM) and comparable to that of etravirine (ETV, EC_{50} = 0.004, 0.014 μM). Molecular docking experiments on the novel analogues have also suggested that the extensive network of main chain hydrogen bonds are important in the binding mode, which may provide valuable insights for further optimization.

Keywords: HIV-1, NNRTIs, DAPY, thiophene[3,2-*d*]pyrimidine, solvent-exposed region I

1. Introduction

HIV-1 non-nucleoside reverse transcriptase inhibitors (NNRTIs) comprise an important class of antiretroviral drugs, and combinations of NNRTIs are widely used in highly active antiretroviral therapy (HAART) regimens to treat HIV infection in view of their potent antiviral activity, high selectivity, and favorable pharmacokinetics.[1, 2] Currently, there are five FDA-approved NNRTIs administered as a combination therapy in HAART, including the first generation NNRTIs nevirapine (NVP), efavirenz (EFV), delavirdine (DLV) and the second generation NNRTIs etravirine (ETV, **1**) and rilpivirine (PRV, **2**)[3, 4] (**Figure 1**). Although HAART has greatly reduced the morbidity and mortality of AIDS, the increasing incidence of drug resistant continues being a major cause of treatment failure[5]. Among all the mutant strains, K103N and Y181C are the two most prevalent mutations selected by NVP

and EFV[6], E138K are the mutant strains most frequently selected by RPV[7]. In addition, hypersensitivity reactions and some other drug toxicity have been reported with second generation NNRTIs[8]. Therefore, searching for novel chemical skeletons with improved drug resistance profiles is actively pursed.

According to a wide range of co-crystal structures of HIV-1 reverse transcriptase (RT)/NNRTIs complexes[9, 10], the diarylpyrimidines (DAPY) derivatives featured a similar pharmacodynamics interactions: 1) the left aryl wing develops hydrophobic interaction with Tyr181, Tyr188, Phe227 and Trp229; 2) the NH linker between the central pyrimidine and the right wing and the N atom of the pyrimidine participates in the conserved hydrogen bonds with the backbone of Lys101; 3) the right wing forms extensive interactions with the surrounding lipophilic sub-pocket defined by Val106, Pro236, and Tyr318, which was named the "solvent-exposed region I". In the structure-based lead optimization phase of drug development, solvent-exposed protein regions are known as prospective sites for modification for the reason that they have larger spaces to accommodate diverse structures with different structures and electrical properties, which contribute to achieve additional and specific protein-ligand interactions with the target protein. Thus, exploiting solvent-exposed regions is becoming more conventional strategy for enhancing binding affinity, improving potency, and overcoming drug resistance profiles.

Previous research efforts in our lab for exploiting the solvent-exposed regions of HIV-1 RT achieved the discovery of piperidine-substituted thiophene[3,2-*d*]pyrimidine K-5a2, which exhibited broad-spectrum activity with single-digit nanomolar EC_{50} values against a panel of wild-type (WT) and mutant HIV-1 strains[11-13]. Furthermore, subsequent structural exploration was focus on the solvent-exposed region I of the NNRTIs binding pocket (NNIBP) and the 4-aminopiperidine moiety of the K-5a2 was replaced with cyclohexanediamine, resulting in a conclusion that the linker between the cyclohexanediamine and aryl group exhibited significant influence to anti-HIV-1 activity

(**Figure 2**). The sulfamide linker was turned to be the most efficient privilege structure [14, 15]. Compound **ACS-9d** proved to be the most effective inhibitor and exhibited single-figure-nanomolar activity (EC_{50} = 7.1 nM) against WT HIV-1 strain. However, **ACS-9d** showed decreased activities against other single and double mutant strains compared to ETV. With the aim to further explore the structure-activity relationship (SAR) of the right wing and generate more effective inhibitors with improved potency against resistance-associated variants, we designed subseries-**5** with the strategy of molecular hybridization by introducing the sulfonamide linker to the aminopiperidine of the K-5a2. The subseries-**8** was designed based on the strategy of scaffold hopping, by replacing the cyclohexane ring with benzene ring. Substituents with structural diversity were introduced to the sulfamide linker and point to the solvent-exposed region I. We hope the newly introduce sulfamide linker and substituents could develop additional interactions with the amino acid in solvent-exposed region I and improve activities against mutant HIV-1 strains.

In this study, we report the synthesis, antiviral activity and molecular simulation of the newly designed compounds. Preliminary SARs are also discussed in detail to gain further insights into this series of analogues.

2. Results and discussion

2.1 Chemistry

The synthetic protocols for the novel designed derivatives are outlined in **Schemes 1−2.** As depicted in **Scheme 1**, the synthetic sequence started from 2,4-dichlorothiophene[3,2-*d*]pyrimidine with 3,5-dimethyl-4-hydroxybenzonitrile in dimethyl formamide (DMF) to give **2**. Subsequently, treatment of **2** with 4-(*tert*-butoxycarbonyl)aminopiperidine brought **3** *via* nucleophilic substitution. Remove the t-butyloxycarboryl (Boc) protective group of **3** with trifluoroacetic acid (TFA) in dichloromethane (DCM) gave **4**, followed by acylation reaction in the presence of substituted sulfonyl chloride to achieve the target compounds **5a-k**. The synthetic routes for target

compounds **8a-i** was similar to that of **5a-k**, with the difference that the intermediate **6** was obtained by Buchwald-Hartwig cross coupling reaction of **2** with *tert*-butyl (4-aminophenyl)carbamate in the presence of (±)-2,2'-bis(diphenylphosphino)-1,1'-binaphthalene (BINAP) and $PdCl_2(PPh_3)_2$ (**Scheme 2**).

2.2 Biological evaluations

The antiviral potency of the newly synthesized derivatives were evaluated in MT-4 cell cultures infected with WT HIV-1 strain (IIIB), NNRTI-resistant single-mutant strains L100I, K103N, Y181C, Y188L, E138K and double-mutant strains F227L+V106A and K103N+Y181C (RES056). Nevirapine (NVP) and Etravirine (ETV) were selected as control drugs[12]. The results were expressed as EC_{50} (anti-HIV potency), CC_{50} (cytotoxicity) and SI (selectivity index, CC_{50}/EC_{50} ratio) (**Tables 1** and **2**).

As depicted in **Table 1**, all the compounds exhibited effective potency against WT HIV-1 with EC_{50} value from micromolar to submicromolar (EC_{50} = 0.058-3.60 μM), with an exception of **8f** (EC_{50} = 12.55 μM). Among them, **7** (EC_{50} = 0.058 μM) and **8b** (EC_{50} = 0.066 μM) were proved to be the most potent inhibitors, being about 5-fold more potent than NVP (EC_{50} = 0.31 μM), but their activities less potent than that of ETV (EC_{50} = 0.004 μM). All compounds were inactive to HIV-2.

Preliminary SAR analysis demonstrated that incorporation of sulfuryl group to the right wing (aniline and piperidine) could result in a decreased activity of the compounds and the bulky substituent group appeared to have a more negative effect on the potency, such as compounds **8f** (EC_{50} = 12.55 μM) and **8h** (EC_{50} = 3.60 μM).

Next, the anti-mutant HIV-1 activities were investigated. As depicted in **Table 2**, all the target compounds exhibited moderate potency against single mutant HIV-1 strains (L100I, K103N, Y181C, Y188L, and E138K) and double mutant HIV-1 strain F227L+V106A, but all of them lost their activity to double mutant strain RES056. A brief investigation of SARs revealed that the activity of the compounds against mutant HIV-1 strains was consistent with that against WT HIV-1 virus. Compounds **7** (EC_{50} = 0.014-0.77 μM) and **8b** (EC_{50} = 0.044-2.77 μM) inhibited most common single mutations and double mutations F227L+V106A in the micromolar concentration range. More encouragingly, the results demonstrated that their activity to mutant strains K103N and E138K, was superior to the activity against WT HIV-1 strain. Especially, the activity of **7** (EC_{50} = 0.014, 0.031 μM) was more effective than that of NVP (EC_{50} = 7.57, 0.19 μM) and comparable to that of ETV (EC_{50} = 0.004, 0.014 μM) toward the two mutations, which could be regarded as promising lead compound for drug discovery overcoming the drug resistance profiles.

2.3 Molecular modeling analysis

To shed light on the binding modes of these novel thiophene[3,2-*d*]pyrimidine derivatives, the representative compound **8b** was docked into the WT HIV-1 NNRTIs binding pocket (PDB code: 3MEC[10]) and K103N mutant NNRTIs binding pocket (PDB code: 3MED[10]) using the software SurflexeDock SYBYL-X 2.0. PyMOL was used to visualize the results. The docking protocol was same with our established method previously[12].

As shown in **Figure 3A**, **8b** adopted a typically horseshoe-like conformation in the NNIBP, the binding mode was similar to that of the lead compound, featuring mainly well-known pharmacophoric interactions: (i) The left wing structure (4-cyano-2,6-dimethylphenoxy) of **8b** occupied the hydrophobic subpocket formed by aromatic amino acid residues Tyr181, Tyr188, Phe227 and Trp229, developing hydrophobic

interactions with these amino acid residues; (ii) The right piperidine ring of **8b** formed close van der Waals interactions with the lipophilic side chains of Lys103, Val106, Phe227, and Pro236; (iii) NH linker connecting the central pyridine ring and the piperidine ring formed a conserved hydrogen bond with the backbone of Lys101.

In addition, the newly introduced thiophene ring project into the entrance tunnel surrounded by Val179 and Glu138, and the sulphur atom establish p-π interactions with them; the benzene-linked sulfuric diamide group develops hydrogen-bonding interactions with the backbone of His235 as hydrogen bond donor, providing a rational explanation of the relatively improved activity of **8b** compared to other compounds. However, compared with ETV, **8b** lost the crucial hydrogen-bonding interaction between the *N* atom of the thiophene[3,2-*d*]pyrimidine and the backbone of Lys101, which account for its decreased potency.

When the Lys103 mutates into Asn103 (K103N) (**Figure 3B**), the binding mode of **8b** with K103N RT was similar to that with WT RT, only with the difference that sulfuric diamide group develops double hydrogen-bonding interactions with the backbone of His235 and Tyr318, which probably plays an essential role in improving its activity against the K103N mutant than WT HIV-1.

2.4 *In silico* prediction of physicochemical properties

Furthermore, the potent compounds **7** and **8b** were predicted their druglikeness features using the free on-line software molinspiration (http://www.molinspiration.com/)[13]. As depicted in **Table 3**, the molecular weight (MW), hydrogen bond acceptors (nON), hydrogen bond donors (nOHNH), rotatable bonds (nrotb), and Logp of the compounds **7** and **8b** abide by the Lipinski's rule of five, with an exception of the Log P of the **7** over the limit value (Log P = 5.07). In addition, Lipophilic parameter ligand efficiency (LE) and Ligand

efficiency dependent lipophilic (LELP) were also calculated and conformed well to the rule[16]. Therefore, it is supposed that **7** and **8b** have the desired physicochemical properties for further lead optimization.

3. Conclusion

We have reported herein efforts to exploit the chemical space of solvent-exposed regions I of the NNIBP toward generate more effective inhibitors with improved drug resistance profiles. Based on the molecular hybridization and scaffold hopping strategy, a series of novel DAPY derivatives was designed. Most of them showed moderate to excellent potency against WT HIV-1 strain, compounds **7** and **8b** proved to be the most potent inhibitors with EC_{50} value of 0.058 and 0.066μM, respectively. Notably, compound **7** was demonstrated with more active potency against the single mutant HIV-1 strains K103N and E138K (EC_{50} = 0.014 and 0.031 μM, respectively), being comparable to that of ETV (EC_{50} = 0.004, 0.014 μM). Furthermore, molecular simulation analysis suggested that the double hydrogen-bonding interactions between the sulfuric diamide group and the backbone of His235 and Tyr318 contribute to the improved drug resistance profiles. Further optimization of the scaffold is currently underway and will be reported in due course.

Supporting information

Supportinng Information including the synthetic produce and spectral data of the target compounds.

Notes

The authors declare no competing financial interest.

Acknowledgements

We gratefully acknowledge financial support from the National Natural Science Foundation of China (NSFC Nos. 81420108027, 81573347), Young Scholars Program of Shandong University (YSPSDU No. 2016WLJH32), the Fundamental Research Funds of Shandong University (No. 2017JC006), and Key research and development project of Shandong Province (No. 2017CXGC1401) and KU Leuven (GOA 10/014).

List of the figure legends

Figure 1: Chemical structures of next-generation NNRTI drugs.

Figure 2. Rational design of target compounds by employing molecular hybridization and scaffold hopping strategy.

Figure 3. (A) Predicted binding mode of **8b** with the HIV-1 WT RT (PDB: 3MEC); (B) Predicted binding mode of **8b** with the HIV-1 K103N RT (PDB: 3MED); Hydrogen bonds are indicated with dashed lines (yellow). Nonpolar-hydrogen atoms are not shown for clarity.

Scheme 1. Synthesis of target compounds 5a-k. Reagents and conditions: (i) 3,5-dimethyl-4-hydroxybenzonitrile, DMF, K_2CO_3, r.t.; (ii) 4-(*tert*-butoxycarbonyl)aminopiperidine, DMF, K_2CO_3, 120°C; (iii) TFA, DCM, r.t.; (iv) substituted sulfonyl chloride, DCM, Et_3N, 0°C to r.t.

Scheme 2. Synthesis of target compounds 8a-i. Reagents and conditions: (i) 3,5-dimethyl-4-hydroxybenzonitrile, DMF, K_2CO_3, r.t.; (ii) *tert*-butyl (4-aminophenyl)carbamate, BINAP, $PdCl_2(PPh_3)_2$, Cs_2CO_3, 1,4-dioxane, 120°C; (iii) TFA, DCM, r.t.; (iv) substituted sulfonyl chloride, DCM, Et_3N, 0°C to r.t.

Table 1. Anti-HIV activity against HIV-1 (IIIB) and RES056 strains and cytotoxicity of **5a-k**, **7** and **8a-i**

Table 2. Anti-HIV-1 activity against mutant strains and cytotoxicity

Table 3. Physicochemical properties and LE, LELP of **7** and **8b**

References

[1] P. Zhan, C. Pannecouque, E. De Clercq and X. Liu. Anti-HIV Drug Discovery and Development: Current Innovations and Future Trends. Journal of medicinal chemistry. 2016, 59: 2849-2878.

[2] R. J. Shattock, M. Warren, S. Mccormack and C. A. Hankins. AIDS. Turning the tide against HIV. Science (New York, N.Y.). 2011, 333: 42-43.

[3] X. Chen, P. Zhan, D. Li, C. E. De and X. Liu. Recent advances in DAPYs and related analogues as HIV-1 NNRTIs. Current medicinal chemistry. 2011, 18: -.

[4] C. E. De and G. Li. Approved Antiviral Drugs over the Past 50 Years. Clinical Microbiology Reviews. 2016, 29: 695.

[5] R. K. Gupta, J. Gregson, N. Parkin, H. Haile-Selassie, A. Tanuri, F. L. Andrade, P. Kaleebu, C. Watera, A. Aghokeng and N. Mutenda. HIV-1 drug resistance before initiation or re-initiation of first-line antiretroviral therapy in low-income and middle-income countries: a systematic review and meta-regression analysis. Lancet Infectious Diseases. 2017.

[6] J. A. Johnson, J. F. Li, L. Morris, N. Martinson, G. Gray, J. Mcintyre and W. Heneine. Emergence of drug-resistant HIV-1 after intrapartum administration of single-dose nevirapine is substantially underestimated. Journal of Infectious Diseases. 2005, 192: 16-23.

[7] G. Bec, B. Meyer, M. A. Gerard, J. Steger, K. Fauster, P. Wolff, D. Burnouf, R. Micura, P. Dumas and E. Ennifar. Thermodynamics of HIV-1 reverse transcriptase in action elucidates the mechanism of action of non-nucleoside inhibitors. Journal of the American Chemical Society. 2013, 135: 9743-9752.

[8] M. J. Feinstein, C. J. Achenbach, N. J. Stone and D. M. Lloydjones. A Systematic Review of the Usefulness of Statin Therapy in HIV-Infected Patients. American Journal of Cardiology. 2015, 115: 1760-1766.

[9] K. Das, J. D. Bauman, A. D. Clark, Jr, Y. V. Frenkel, P. J. Lewi, A. J. Shatkin, S. H. Hughes and E. Arnold. High-resolution structures of HIV-1 reverse transcriptase/TMC278 complexes: strategic flexibility explains potency against resistance mutations. Proceedings of the National Academy of Sciences of the United States of America. 2008, 105: 1466-1471.

[10] E. B. Lansdon, K. M. Brendza, M. Hung, R. Wang, S. Mukund, D. Jin, G. Birkus, N. Kutty and X. Liu. Crystal structures of HIV-1 reverse transcriptase with etravirine (TMC125) and rilpivirine (TMC278): implications for drug design. Journal of medicinal chemistry. 2010, 53: 4295-4299.

[11] D. Kang, Z. Fang, Z. Li, B. Huang, H. Zhang, X. Lu, H. Xu, Z. Zhou, X. Ding, D. Daelemans, E. De Clercq, C. Pannecouque, P. Zhan and X. Liu. Design, Synthesis, and Evaluation of Thiophene[3,2-d]pyrimidine Derivatives as HIV-1 Non-nucleoside Reverse Transcriptase Inhibitors with Significantly Improved Drug Resistance Profiles. Journal of medicinal chemistry. 2016, 59: 7991-8007.

[12] D. Kang, Z. Fang, B. Huang, X. Lu, H. Zhang, H. Xu, Z. Huo, Z. Zhou, Z. Yu, Q. Meng, G. Wu, X. Ding, Y. Tian, D. Daelemans, E. De Clercq, C. Pannecouque and P. Zhan. Structure-Based Optimization of Thiophene[3,2-d]pyrimidine Derivatives as Potent HIV-1 Non-nucleoside Reverse Transcriptase Inhibitors with Improved Potency against Resistance-Associated Variants. Journal of medicinal chemistry. 2017, 60: 4424-4443.

[13] Z. Huo, H. Zhang, D. Kang, Z. Zhou, G. Wu, S. Desta, X. Zuo, Z. Wang, L. Jing, X. Ding, D. Daelemans, E. De Clercq, C. Pannecouque, P. Zhan and X. Liu. Discovery of Novel Diarylpyrimidine Derivatives as Potent HIV-1 NNRTIs Targeting the "NNRTI Adjacent" Binding Site. ACS medicinal chemistry letters. 2018, 9: 334-338.

[14] D. Kang, X. Ding, G. Wu, Z. Huo, Z. Zhou, T. Zhao, D. Feng, Z. Wang, Y. Tian, D. Daelemans, E. De Clercq, C. Pannecouque, P. Zhan and X. Liu. Discovery of Thiophene[3,2-d]pyrimidine Derivatives as Potent HIV-1 NNRTIs Targeting the Tolerant Region I of NNIBP. ACS medicinal chemistry letters. 2017, 8: 1188-1193.

[15] D. Kang, Z. Wang, H. Zhang, G. Wu, T. Zhao, Z. Zhou, Z. Huo, B. Huang, D. Feng, X. Ding, J. Zhang, X. Zuo, L. Jing, W. Luo, S. Guma, D. Daelemans, E. Clercq, C. Pannecouque, P. Zhan and X. Liu. Further Exploring Solvent-Exposed Tolerant Regions of Allosteric Binding Pocket for Novel HIV-1 NNRTIs Discovery. ACS medicinal chemistry letters. 2018, 9: 370-375.

[16] A. L. Hopkins, C. R. Groom and A. Alex. Ligand efficiency: a useful metric for lead selection. Drug Discov Today. 2004, 9: 430-431.

Graphical Table of Contents

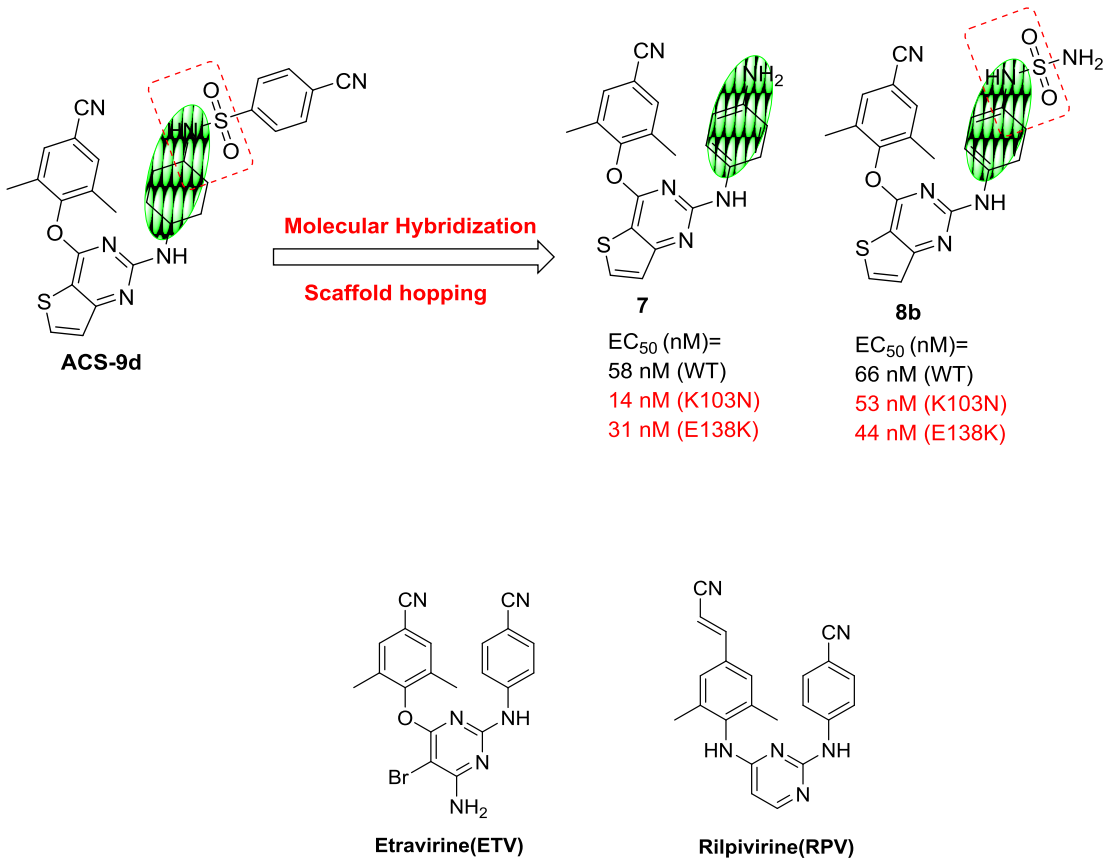

Figure 1: Chemical structures of next-generation NNRTI drugs

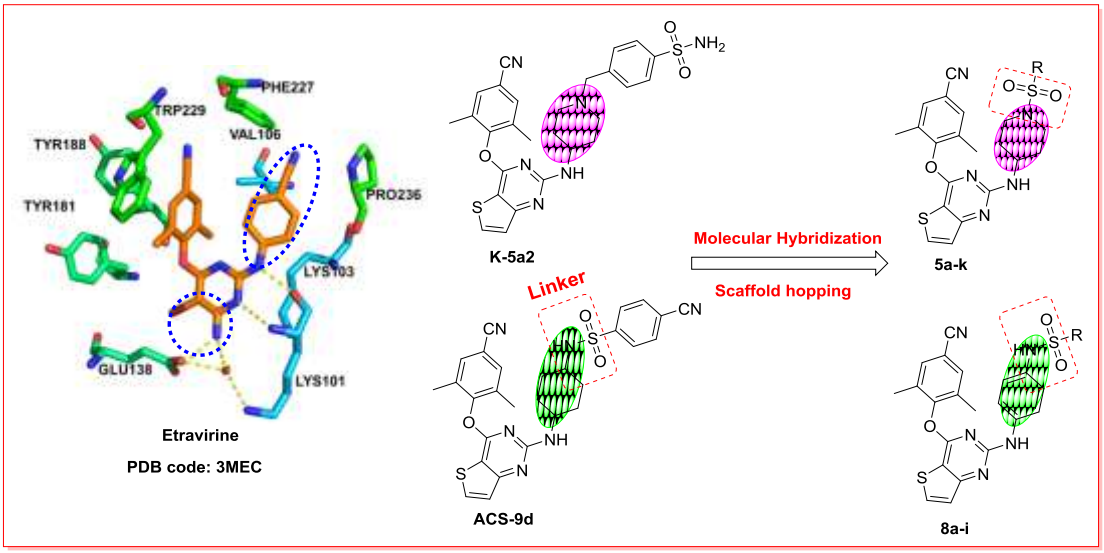

Figure 2. Rational design of target compounds by employing molecular hybridization and scaffold hopping strategy.

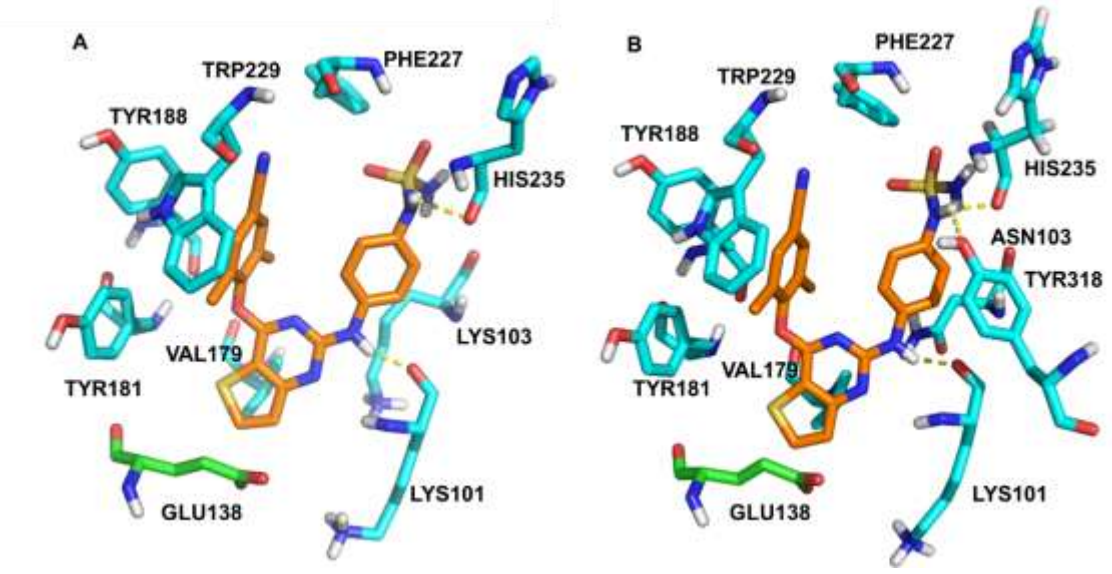

Figure 3. (A) Predicted binding mode of **8b** with the HIV-1 WT RT (PDB: 3MEC); (B) Predicted binding mode of **8b** with the HIV-1 K103N RT (PDB: 3MED); Hydrogen bonds are indicated with dashed lines (yellow). Nonpolar-hydrogen atoms are not shown for clarity.

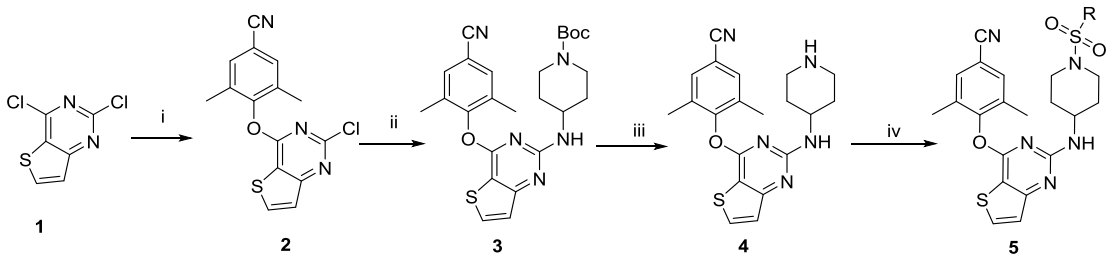

Scheme 1. Reagents and conditions: (i) 3,5-dimethyl-4-hydroxybenzonitrile, DMF, K_2CO_3, r.t.; (ii) 4-(*tert*-butoxycarbonyl)aminopiperidine, DMF, K_2CO_3, 120°C; (iii) TFA, DCM, r.t.; (iv) substituted sulfonyl chloride, DCM, Et_3N, 0°C to r.t.

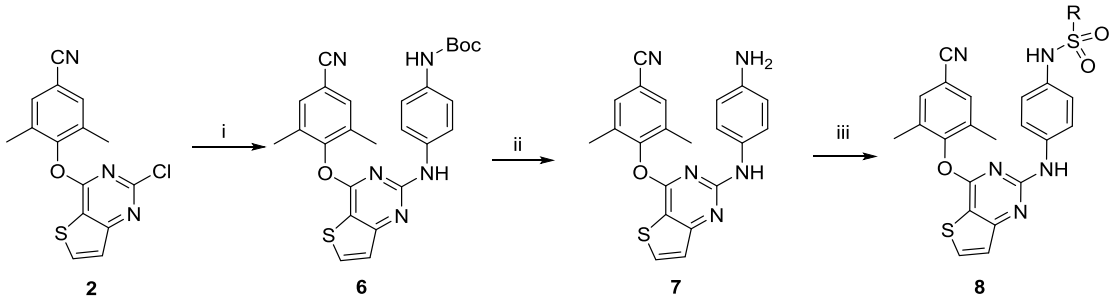

Scheme 2. Reagents and conditions: (i) 3,5-dimethyl-4-hydroxybenzonitrile, DMF, K_2CO_3, r.t.; (ii) *tert*-butyl (4-aminophenyl)carbamate, BINAP, $PdCl_2(PPh_3)_2$, Cs_2CO_3, 1,4-dioxane, 120°C; (iii) TFA, DCM, r.t.; (iv) substituted sulfonyl chloride, DCM, Et_3N, 0°C to r.t.

Table 1. Anti-HIV activity against HIV-1 (IIIB) and RES056 strains and cytotoxicity of **5a-k**, **7** and **8a-i**

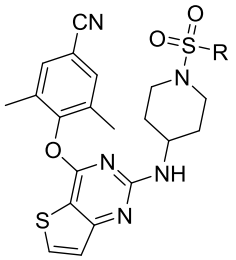

5a-k

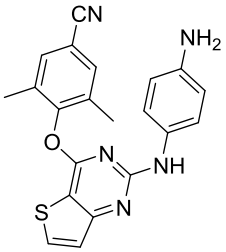

7

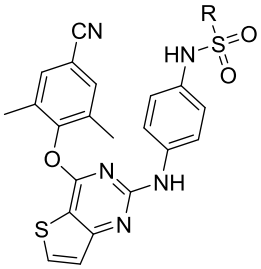

8a-i

Compds	R	EC_{50} (μM)[a]		CC_{50} (μM)[b]	SI (IIIB)[c]
		IIIB	ROD		
5a	CH_3	0.58±0.065	>22.21	22.21±7.48	39
5b		0.35±0.143	>6.185	6.19±2.37	18
5c	NH_2	0.24±0.089	>20.35	20.35±7.119	84
5d	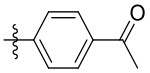	0.33±0.109	>21.98	21.98±13.99	67
5e	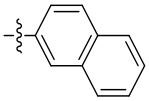	0.74±0.65	>219.4	>219.4	>295
5f	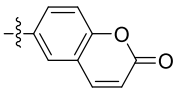	0.29±0.11	>56.92	56.92±51.34	193
5g	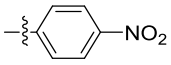	0.85±0.45	>81.73	81.73±66.46	96
5h	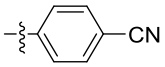	0.44±0.28	>20.98	20.98±13.94	48
5i	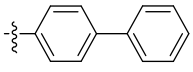	1.10±0.54	>209.8	>209.8	>191
5j	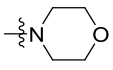	0.22±0.12	>236.4	>236.4	>1059

5k	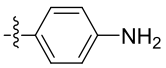	1.35±0.59	>233.79	>233.7	>173
7	-	0.058±0.029	>19.39	19.39±12.60	335
8a	CH_3	1.77±0.61	>268.4	>268.4	>151
8b	NH_2	0.066±0.019	>25.06	25.06±5.24	378
8c		0.58±0.54	>19.65	19.65±11.73	34
8d	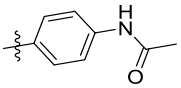	0.28±0.071	>12.664	12.66±6.60	45
8e	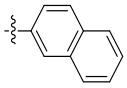	1.17±0.36	>216.3	>216.3	>185
8f	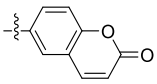	12.55±2.04	>209.8	>209.8	>17
8g	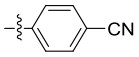	0.32±0.085	>46.73	46.73±24.64	148
8h	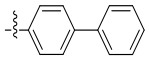	3.60±1.11	>207.0	>207.0	>57
8i	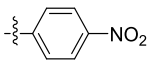	1.35±0.32	>91.40	91.40±61.02	68
NVP	-	0.31±0.056	>7.590	>15.02	>48.08
ETV	-	0.004±0.001	>4.585	>4.585	>1818

[a] EC_{50}: concentration of compound required to achieve 50% protection of MT-4 cell cultures against HIV-1-induced cytotoxicity, as determined by the MTT method. A smaller number means that the compound has a higher activity.

[b] CC_{50}: concentration required to reduce the viability of mock-infected cell cultures by 50%, as determined by the MTT method. A larger number means that the compound has a lower toxicity.

[c] SI: selectivity index, the ratio of CC_{50}/EC_{50}.

Table 2. Anti-HIV-1 activity against mutant strains and cytotoxicity

Compds	EC_{50} (μM)						
	L100I	**K103N**	**Y181C**	**Y188L**	**E138K**	**F227L+V106A**	**RES056**
5a	4.26±0.45	0.31±0.073	6.30±0.366	6.60±0.97	0.31±0.089	2.88±1.13	>22.21
5b	≥8.83	0.48±0.077	>6.19	>6.19	0.26±0.056	>6.185	>6.185
5c	4.16±0.99	0.30±0.047	4.72±0.82	5.96±1.61	0.21±0.033	3.67±0.12	>20.35
5d	10.29±9.928	0.48±0.27	≥16.73	≥15.18	0.40±0.075	≥15.18	>21.98
5e	4.09±1.59	0.37±0.01	4.78±0.40	3.42±0.64	0.72±0.039	29.43±13.47	>219.4
5f	1.87±0.005	0.15±0.021	0.76±0.013	1.04±0.107	0.23±0.040	≥30.08	>56.92
5g	9.23±1.97	0.54±0.18	6.17±0.75	10.73±3.87	0.77±0.056	7.93±0.51	>81.73
5h	4.32±0.25	0.57±0.13	3.73±0.045	5.78±1.849	0.66±0.095	5.73±1.56	>20.98
5i	191.7±21.50	3.21±0.005	146.5±44.75	171.1±47.31	0.59±0.037	177.7±15.25	>209.8
5j	41.31±25.63	0.57±0.075	64.55±15.76	126.2±9.123	0.056±0.017	59.42±14.48	>236.4
5k	14.18±1.863	1.98±0.541	17.33±0.005	≥35.51	3.12±0.024	>233.7	>233.79
7	0.28±0.061	0.014±0.001	0.78±0.009	0.79±0.043	0.031±0.004	0.77±0.11	>19.39
8a	17.91±0.32	2.11±0.61	33.79±2.612	23.81±1.74	1.18±0.34	4.19±1.95	>268.4
8b	0.71±0.083	0.053±0.007	1.69±0.27	2.77±0.38	0.044±0.005	0.24±0.092	>25.06
8c	2.03±0.48	0.33±0.062	4.82±0.165	7.74±0.98	0.44±0.20	6.04±0.45	>19.65
8d	2.89±2.15	0.14±0.071	5.86±0.23	≥7.15	0.33±0.025	4.60±1.49	>12.66
8e	5.53±0.90	0.98±0.089	110.1±19.63	127.8±26.30	1.58±0.25	57.82±8.26	>216.3
8f	108.7±10.70	7.49±1.06	>209.8	>209.8	31.15±2.812	>209.8	>209.8
8g	1.63±0.35	0.20±0.035	5.43±0.63	6.69±0.54	0.38±0.12	4.14±0.31	>46.73
8h	52.79±4.17	2.75±0.30	>207.0	>207.0	4.93±1.74	≥163.8	>207.0
8i	3.45±0.11	0.86±0.38	36.81±5.91	41.04±1.16	1.93±0.048	7.86±0.789	>91.40
NVP	0.74±0.17	7.53±0.22	-	-	0.19±0.087	-	>7.59
ETV	0.010±0.003	0.004±0.001	0.019±0.007	0.020±0.003	0.014±0.002	0.023±0.011	0.25±0.001

Table 3. Physicochemical properties and LE, LELP of **7** and **8b**

Compd	MW	nON[a]	nOHNH[a]	nrotb[a]	LogP[a]	LE[b]	LELP[c]
Accepted range	< 500	< 10	< 5	≤ 10	< 5	> 0.3	< 16.5
7	335.91	6	3	4	5.07	0.34	14.53
8b	466.55	9	4	6	4.61	0.31	15.21

[a] Using free on-line software (http://www.molinspiration.com/);

[b]LE = calculated by the formula −ΔG/HA (non- hydrogen atom), ΔG = RT ln Kd, pre-suming Kd ≈ EC_{50} (IIIB); R= 1.987 × 10 –3 kcal/K/mol, T = 298 K.

[c] LELP = Log P/LE